NENE
International Conference
Nuclear Energy for New Europe

Development of 3D Fracture Mechanics Submodels for PTS Analyses of an RPV With Cracks

Oriol Costa Garrido, Nejc Kromar, Andrej Prošek, Leon Cizelj
Jožef Stefan Institute
Jamova cesta 39
SI-1000 Ljubljana, Slovenia
oriol.costa@ijs.si, nejc.kromar@ijs.si, andrej.prosek@ijs.si, leon.cizelj@ijs.si

ABSTRACT

A limiting event for an operating nuclear power plant is the so-called pressurized thermal shock (PTS). An integrity analysis of the reactor pressure vessel (RPV) during a PTS event requires the evaluation of temperatures and stresses in the RPV and, subsequently, the computation of stress intensity factors (SIFs) of postulated cracks in the RPV wall. The aim of this paper is to develop and verify a set of three-dimensional (3D) fracture-mechanics submodels with axially and circumferentially oriented, through-clad and embedded, cracks using conventional finite element (FE) method. The developed cracked submodels are employed to compute the SIFs together with the temperatures and stresses obtained with a 3D-FE model of a 4-loop RPV during a selected PTS event. The paper's outcome shows an overall good agreement of the obtained SIFs with available formulae and computer codes.

1 INTRODUCTION

Pressurized thermal shock (PTS) analyses are required to assure that, during the operation of a pressurized water reactor (PWR), potentially existing crack-like flaws in the reactor pressure vessel (RPV) wall will not initiate and propagate during loss-of-coolant-accidents (LOCAs), or other PTS-relevant transient scenarios [1]. A PTS analysis requires a thermo-mechanical analysis to first evaluate the temperatures and stresses in the RPV wall during the transient using, typically, a finite-element (FE) model of the RPV. Then, stress intensity factors (SIFs) of postulated cracks in the RPV wall are computed in fracture mechanics analyses. Finally, the evaluation of the likelihood of crack growth initiation is performed by comparing the SIFs to the fracture toughness of the RPV material.

Semi-analytical formulae of SIFs [2] and dedicated computer codes [3] have been developed in recent years to perform PTS analyses. However, these typically assume a cylindrically shaped RPV, where the heat transfer occurs in the radial (through thickness) direction only, i.e., a one-dimensional (1D) model of the RPV. A costlier and more time-consuming 3D model of the RPV is needed to account for non-homogeneous temperature distributions and/or geometrical discontinuities. A drawback of 3D RPV models that include a postulated crack is that different models of the entire RPV are required to study different crack shapes, sizes and orientations. In addition to the fact that meshing of the cracked region is a rather complex task in itself, the consideration of the relatively small crack also complicates the meshes and increases the number of elements in the overall RPV model. To avoid this, the submodeling technique can be used to perform the analyses [4].

This paper presents the development of 3D fracture-mechanics submodels containing axially and circumferentially oriented through-clad (TCC) and embedded (EMB) cracks. A previously developed 3D FE model of an RPV is employed in the thermo-mechanical analysis of a small-break LOCA (SB-LOCA) [5], presented in Section 2. The developed submodels and

their meshes are described in Section 3, and Section 4 introduces the existing semi-analytical formulae and the FAVOR code, both used for the verification of the submodels' results in Section 5. Finally, the conclusions are drawn in Section 6. This work has been performed in partial fulfilment of the European project APAL (Advanced PTS Analysis for LTO) [6].

2 PTS EVENT AND STRUCTURAL ANALYSIS

Within the APAL project, a 4-loop Kraftwerk Union KWU-1300 PWR – Konvoi German design – plant has been selected for the studies of a PTS event described by a SB-LOCA from a 50 cm^2 break in the hot leg (HL) of loop #1 together with loss of offsite power. The high-pressure safety injection (HPSI) trains in loop #1 and #4 are assumed to be down for maintenance and to fail at the start of the transient, respectively. Therefore, only loops #2 and #3 receive emergency core cooling water from the high-pressure pumps. However, all four loops receive injection from the low-pressure safety injection (LPSI) pumps. The four accumulators (ACCs) connected to cold legs (CLs) are active while the four accumulators connected to HLs are deactivated. The outputs of the thermal-hydraulic analyses [7] with the RELAP5 code [8] are employed as inputs in the structural analysis performed with the ABAQUS code [9]. These include the fluid pressure and the RPV inner surface temperatures available at 8 circumferential locations (4 HLs + 4 CLs) and 11 elevations (from upper head to lower plenum).

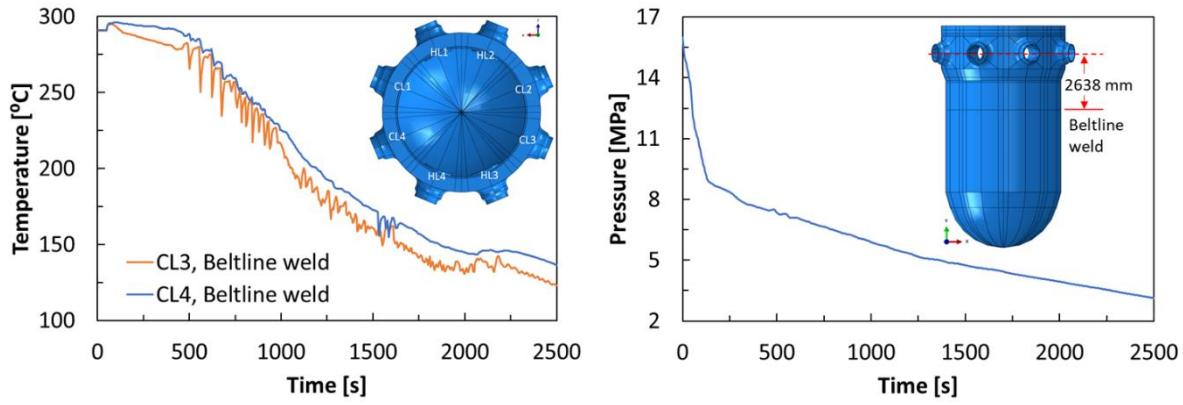

Figure 1: Inner surface temperature of the RPV wall below CL3 and CL4 nozzle centrelines and at the beltline-weld elevation (left) and pressure history at the inner surface of the RPV (right)

Figure 1 shows the pressure history inside the RPV, as well as the temperature histories at two points at the beltline-weld elevation and below CL3 (inside cold plume) and CL4 (outside cold plume) nozzle centrelines. Note that the thermal-hydraulic analyses in APAL have been performed for a transient length of 5000 s and extended to 10000 s [7]. The analyses presented here are however limited to 2500 s as this time is sufficient for the development of the fracture mechanics submodels. The 3D-RPV model and structural analysis are described in detail in Ref. [5]. The model meshes are identical to mesh #4 in [5], with the exception of a remeshing of the lower plenum leading to a total of 136,547 quadratic brick elements of type DC3D20 and C3D20R [9] used, respectively, in the heat transfer and mechanical simulations.

Figure 2 presents the results of the structural analysis at an early time (675 s) into the PTS event. The rather coarse yet non-homogeneous inner surface temperatures (Figure 2-left) depict the development of the cold plume, i.e., a region of colder temperature due to the injection of emergency core cooling water, where high tensile stresses develop (Figure 2-right).

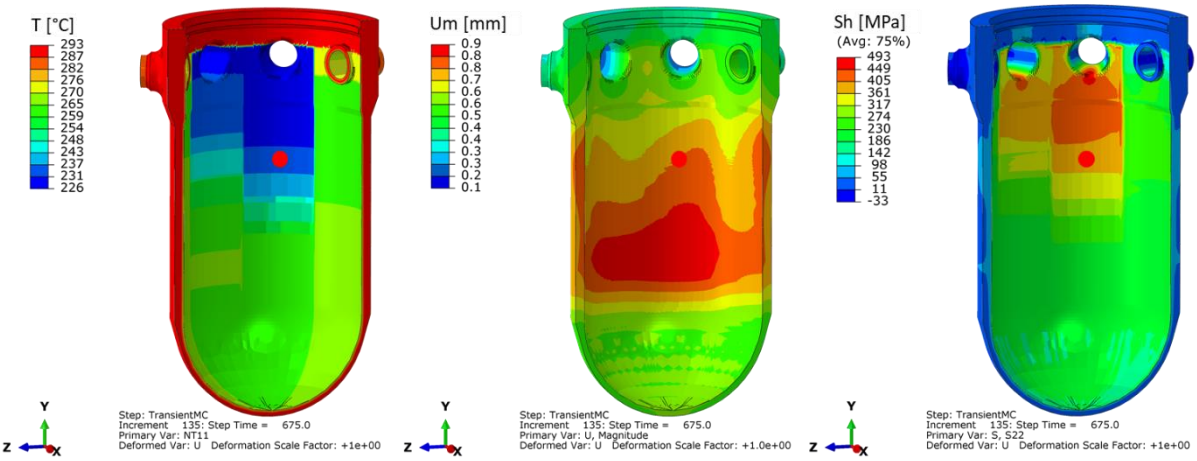

Figure 2: Temperature (left), magnitude of displacements (middle) and hoop stresses (right) in the RPV wall during early stage of cold plume development at time 675 s. The red dot in the 3 figures shows the location below CL3-nozzle centreline and at the beltline-weld elevation

3 FRACTURE-MECHANICS SUBMODELS WITH CRACKS

The submodeling technique relies on the thermo-mechanical (structural) analysis performed with the 3D FE model of the entire RPV without cracks, and submodels of a small portion of the RPV containing the cracks which are used independently in separate fracture-mechanical analyses.

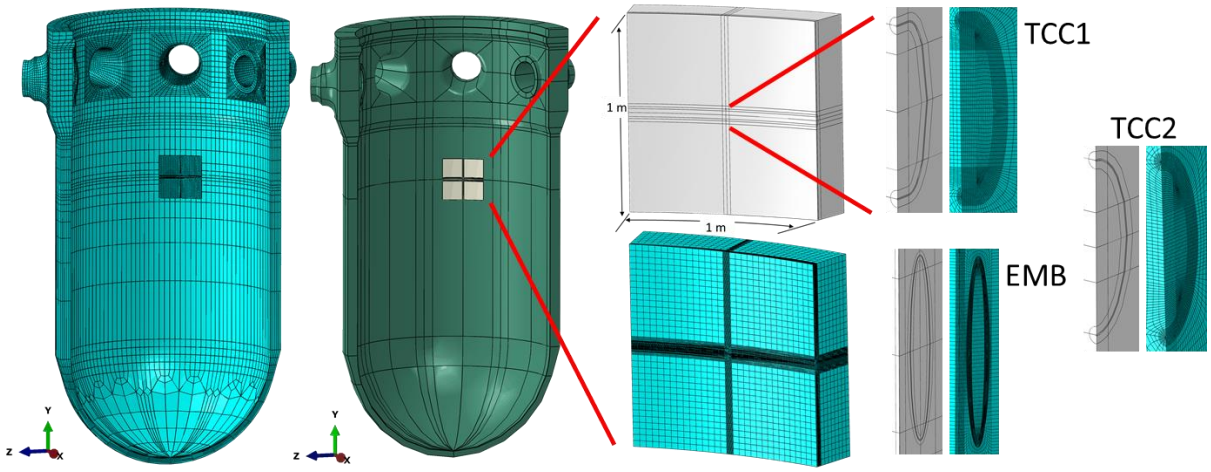

Figure 3: RPV model and fracture-mechanics submodel with the crack located below CL3-nozzle centreline and at the beltline-weld elevation

Figure 3 shows the 3D-RPV model together (for visualization purposes only) with the submodel at the location of interest, i.e., below CL3-nozzle centreline and at the beltline-weld elevation. Six submodels have been developed with the same dimensions of 1 m height and a length along the inner-surface of also 1 m. The submodels include inner-surface breaking semi-elliptical cracks (i.e. through-clad cracks - TCC) of type 1 and 2, and embedded cracks (elliptically shaped within the RPV wall), all of them axially and circumferentially oriented. The major axis of the semi-elliptical TCC1 crack is placed at the boundary between the cladding and base materials and the crack extends straight through the cladding. In TCC2, the major axis is placed on the inner surface of the RPV and the semi-elliptical crack crosses both materials. Figure 4 presents the cracked submodel meshes as well as sketches with the most relevant parameters of the crack geometries and meshes, the values of which are given in Table 1.

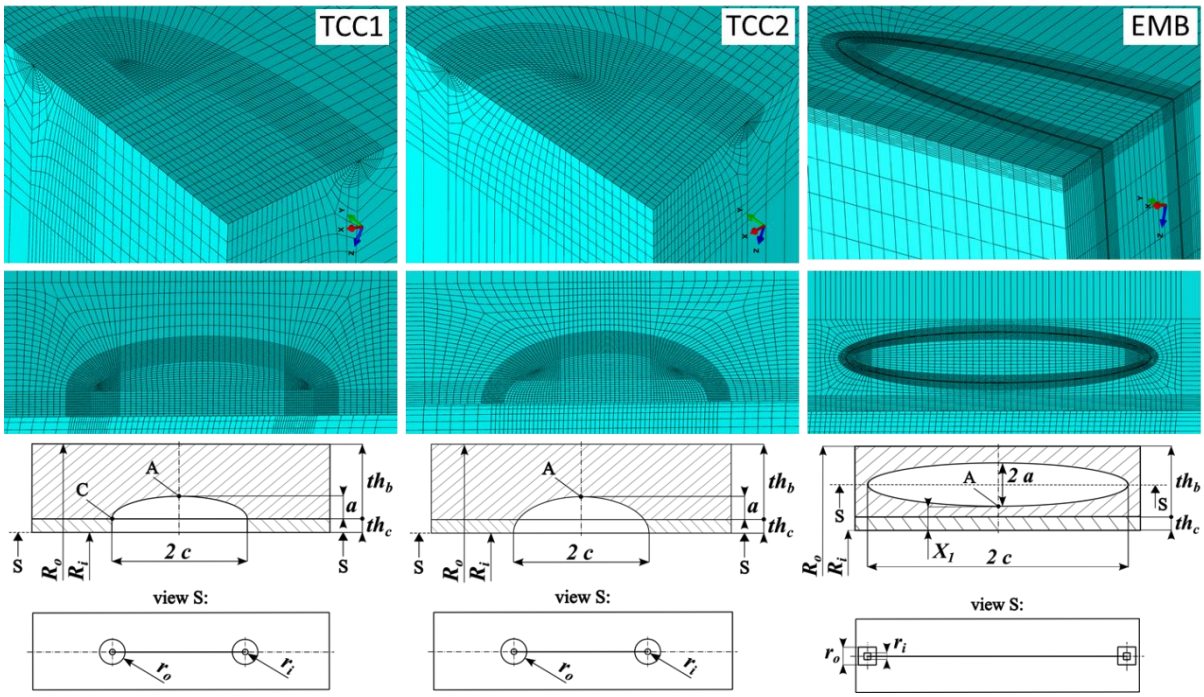

Figure 4: Meshes and sketches of the cracked submodels

In Figure 3 and Figure 4 one can notice that the meshes around the crack line of TCC cracks are circular with wedge elements inside r_i and hexahedral elements inside r_o. The meshes in EMB cracks are square with hexahedral elements only. Another detail is that the 2c dimension in TCC circumferential cracks is placed at the boundary between cladding and base materials (TCC1) or at the inner surface of the RPV (TCC2), thus the major axis of the crack is slightly shorter than 2c. Relevant dimensions of the RPV cylindrical part are the inner and outer radii, respectively, of R_i = 2435 mm and R_o = 2684 mm. The wall thickness consists of a 6 mm austenitic-steel cladding (th_c) and 243 mm ferritic-base material (th_b). Linear-elastic and temperature-dependent material properties from Ref. [5] are assumed.

Table 1: Number of elements and relevant dimensions of submodels with cracks

NUMBER OF ELEMENTS				
Model Type	Whole submodel	Radial (in ri+ro)	Around crack line	Cladding thickness
TCC1	170160	10 (1+9)	16	10
TCC2	161404	10 (1+9)	16	10
EMB	475200	11 (2+9)	4	10

ADDITIONAL INFORMATION						
Bulk elem. avg.size [mm]	*a* [mm]	2c [mm]	X_1 [mm]	ri [mm]	ro [mm]	Singularity controls
~30	10	60	-	0.3	3	Colapsed element side, single node, t=0.25
~30	10	60	-	0.3	3	Colapsed element side, single node, t=0.25
~30	10	120	11	0.3	3	No degeneracy, t=0.50

4 NUMERICAL ANALYSES AND VERIFICATION OF CRACK SUBMODELS

In the fracture mechanics analyses, the displacements obtained in the thermo-mechanical analysis at the submodel boundary surfaces (e.g. see Figure 2-middle) are employed as boundary conditions. Additional loads applied on the submodels include the RPV temperatures in the submodel region and the inner-surface pressure.

The mode I SIF results (i.e. K_I) obtained with the 3D cracked submodels are computed using the contour integral method in ABAQUS. The SIF value of the 5th contour around the crack tip are compared with the results using the formulae for TCC1 developed by Commissariat à l'énergie atomique et aux énergies alternatives (CEA) [2], and with the results for TCC2 and EMB using the Fracture Analysis of Vessels – Oak Ridge (FAVOR) code [3].

FAVOR is a dedicated code for PTS (deterministic and probabilistic) analyses. It performs the heat transfer and mechanical analyses to obtain temperature and stress histories in the RPV wall with a 1D RPV wall assumption. The input data includes the surface temperature at the beltline-weld elevation and below CL3 centreline and the fluid pressure given in Figure 1 (with a heat transfer coefficient of 10^6 W/m^{2}K). The SIFs for the TCC2 cracks are then computed by a weight function approach using the timely stress profiles through thickness. These stress profiles are also used to compute SIFs of EMB cracks following the ASME Section XI-Appendix A model, through a linearization of the stress profile over the crack depth. While the exact EMB crack dimensions considered in the APAL project (Table 1) can be requested, FAVOR only considers TCC2 with length (2c) to total depth (a+thc) ratios equal to 2, 6 and 10. The SIF results for the APAL TCC2 ratio of 3.75 (= 60/(6+10)) are obtained by linear interpolation of the values computed by FAVOR.

The timely stress profiles from FAVOR were saved to disk and used to compute TCC1 SIFs with an in-house implementation of the CEA fourmulae [2]. The CEA TCC1 SIF solutions are also based on the weight function approach with appropriate influence coefficients (or shape factors). Linear interpolation of the influence coefficients given in [2] is performed for the TCC1 crack dimensions studied in APAL (Table 1) assuming the Young's modulus ratio between austenitic and ferritic steels of 0.85.

5 RESULTS OF FRACTURE-MECHANICS ANALYSES

An example of the fracture mechanics results using the submodeling technique in ABAQUS for the TCC1-axial crack submodel is shown in Figure 5. The figure also depicts, for visualization purposes only, the outputs of the thermo-mechanical analysis of the RPV at a later time during the PTS event (1835 seconds) together with the submodel at the location of interest.

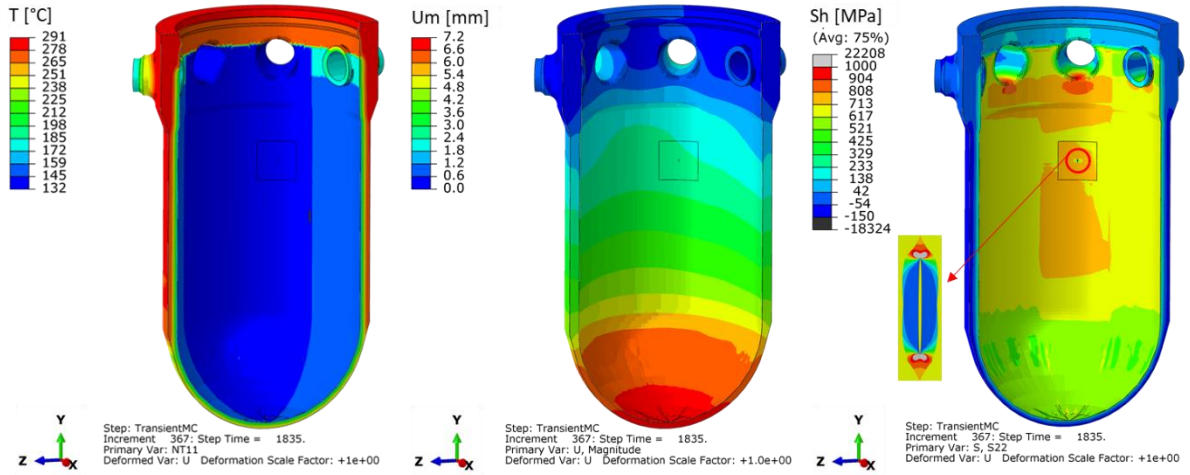

Figure 5: Temperature (left), magnitude of displacements (middle) and hoop stresses (right with TCC1-axial crack inset) in the RPV wall and cracked submodel at time 1835 s, when SIF maxima are reached. In the 3 figures, the submodel is located below CL3-nozzle centreline and beltline-weld elevation

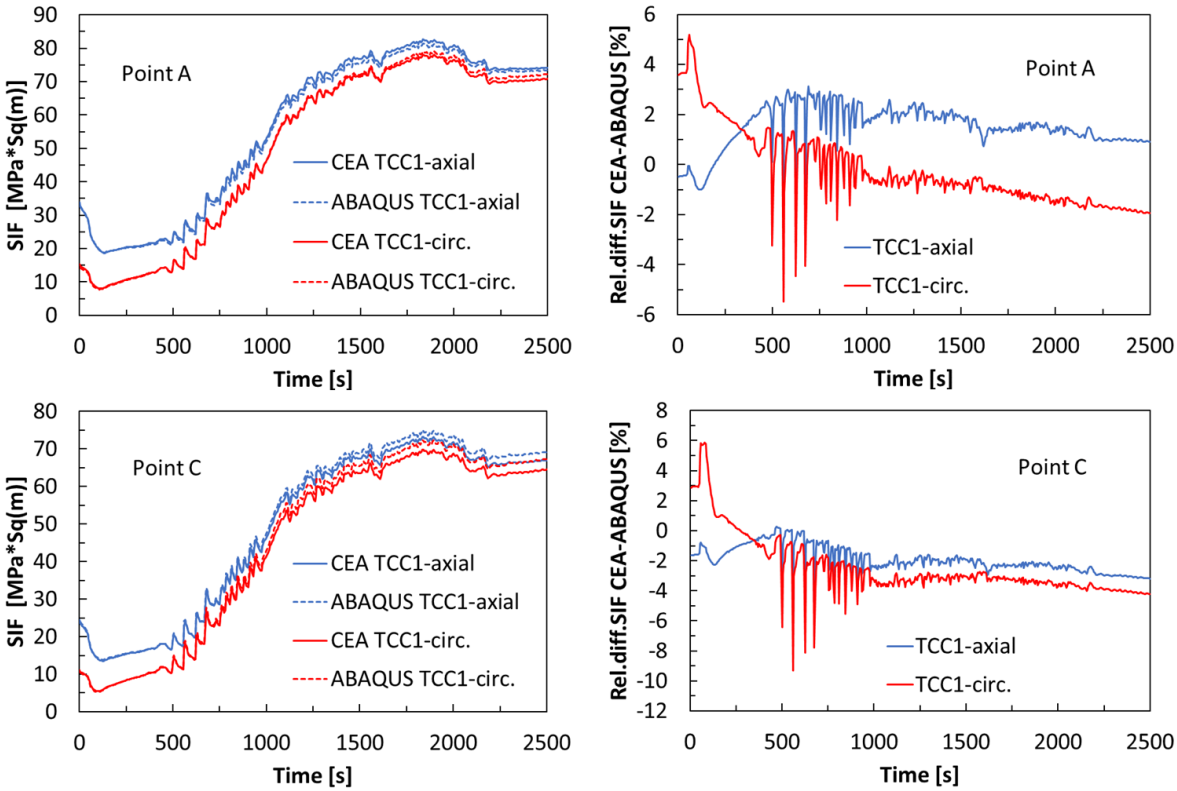

Figure 6: (Left) SIF histories at the deepest point A (top) and at the fusion line C (bottom) of TCC1 (axial and circumferential) cracks obtained with CEA formulae and ABAQUS, and (right) relative difference between the two results

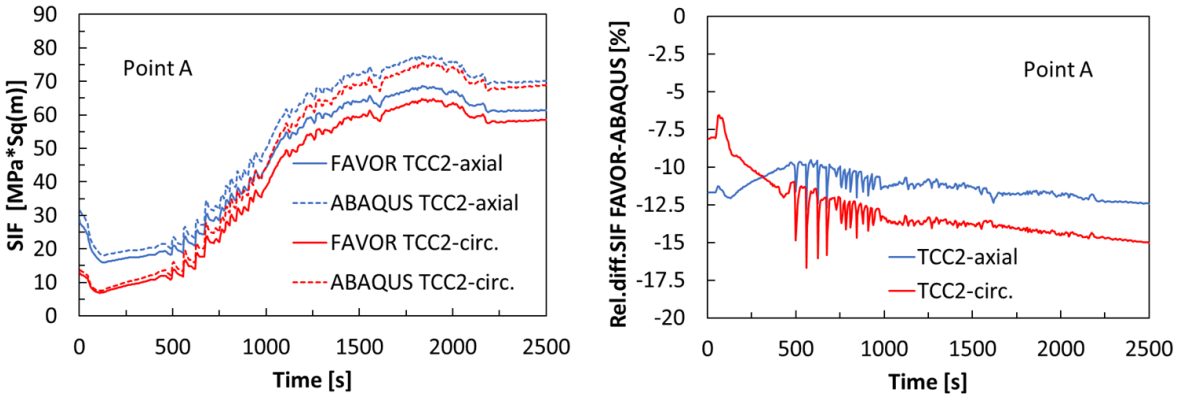

Figure 7: (Left) SIF histories at the deepest point A of TCC2 (axial and circumferential) cracks obtained with FAVOR and ABAQUS and (right) relative difference between the two results

In Figure 5-left and middle one can see the continuous fields of temperatures and displacements at the boundary between the RPV and submodel since they are, respectively, thermal loads and boundary conditions imposed from the RPV to the submodel. However, the crack within the submodel affects the stresses which, in turn, open the crack (see inset in Figure 5-right) due to their tensile nature.

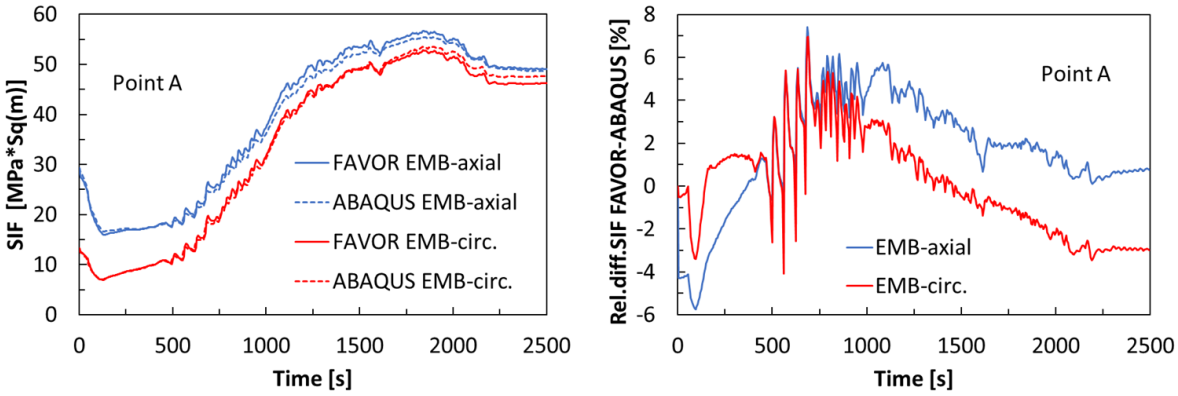

Figure 8: (Left) SIF histories at the deepest point A of embedded (axial and circumferential) cracks obtained with FAVOR and ABAQUS and (right) relative difference between the two results

The SIF results comparison between the ABAQUS submodels and CEA formulae is given in Figure 6 for the TCC1, axial and circumferential, cracks. The figure includes the values of the SIFs at the deepest point A and at the interface point C (see Figure 4), as well as the relative difference between both methods. The TCC1 results show a relative difference of about +/-2% for point A, and about 3% for point C.

Figure 7 presents the SIF results comparison between the ABAQUS submodels and FAVOR for the TCC2, axial and circumferential, cracks at the deepest point A. An absolute difference in SIF of about 10 $\mathrm{MPa}\sqrt{\mathrm{m}}$ leads to the relative difference of about 14%.

The SIF results comparison between the ABAQUS submodels and FAVOR for the EMB, axial and circumferential, cracks are delivered in Figure 8. In this case, a moderate relative difference of about +/-3% is observed, with a peak of about 5%.

Possible source of the discrepancies between the SIFs obtained with the ABAQUS submodels and the formulae and FAVOR is, in all cases, the 3D/1D type of analyses. The linear interpolation of influence coefficients needed to compute SIFs with the CEA formulae for the APAL crack dimensions is another possible source of the observed differences for TCC1. A clear source of the discrepancy for TCC2 is the linear interpolation of the FAVOR SIF results for length-to-total-depth ratios of 2 and 6 at the required value of 3.75. Finally, the linearization of the stress profiles performed by FAVOR may account for some of the small differences observed for EMB cracks. Overall, however, the SIF results obtained with the ABAQUS submodels prove to be in good agreement with the formulae and the FAVOR code.

6 CONCLUSIONS

The paper presents the development and verification of 3D fracture-mechanics submodels in ABAQUS for future PTS analyses. The submodels represent a small portion of the RPV containing through-clad and embedded, axially and circumferentially oriented, cracks. The thermal-hydraulic results with the RELAP5 code of a selected PTS event analysed within the APAL project are used as inputs to perform the thermo-mechanical analysis of the RPV. The results of the structural analysis are subsequently used in the 3D fracture mechanics analyses. The SIF results with the submodels are compared with those obtained with available semi-analytical formulae from CEA and the FAVOR code. Overall, the SIF results with ABAQUS submodels are in good agreement with formulae and FAVOR, and the possible source of the discrepancies, such as 3D/1D type of analyses and interpolations in formulae and FAVOR, are also discussed.

ACKNOWLEDGMENTS

This work has been performed as a part of APAL (Advanced Pressurized Thermal Shock Analysis for Long-Term Operation) project which has received funding from the Euratom research and training programme 2019 - 2020 under grant agreement No 945253. The authors also gratefully acknowledge the financial support of the Slovenian Research Agency through the research program P2-0026. The authors would also like to show their gratitude to the APAL partners from work-packages 2 and 3 for providing the data of their RELAP5 simulations.

REFERENCES

[1] IAEA, "Pressurized Thermal Shock in Nuclear Power Plants: Good Practices for Assessment", IAEA-TECDOC-1627, INTERNATIONAL ATOMIC ENERGY AGENCY, 2010.

[2] S. Marie, S. Chapuliot, "Improvement of the calculation of the stress intensity factors for underclad and through-clad defects in a reactor pressure vessel subjected to a pressurised thermal shock", International Journal of Pressure Vessels and Piping, vol. 85, 2008, pp. 517-531.

[3] P. T. William, et al., Fracture Analysis of Vessels – Oak Ridge FAVOR, v16.1, Computer Code: Theory and Implementation of Algorithms, Methods, and Correlations, ORNL/LTR-2016/309, 2016.

[4] D. F. Mora, et al., "Fracture mechanics analyses of a reactor pressure vessel under non-uniform cooling with a combined TRACE-XFEM approach", Engineering Fracture Mechanics, vol. 238, 2020, pp. 107258.

[5] O. C. Garrido, et al., "Development of a 3D-RPV Finite Element Model for Pressurized Thermal Shock Analyses", International Conference Nuclear Energy for New Europe 2022, Portoroz, Slovenia, 2022.

[6] C. Cueto-Felgueroso, et al., "APAL - Public summary report of WP1 - Deliverable No. D1.6", available from: https://www.apal-project.eu/research-insights, 2021.

[7] P. Kral, et al., "APAL - Public Summary Report of WP2 - Deliverable 2.4", available from: https://www.apal-project.eu/research-insights, 2023.

[8] "RELAP5/MOD3 Code Manual". The RELAP5 Code Development team, NUREG/CR-5535, EG&G Idaho, 1995, pp. Vol.1-7.

[9] ABAQUS, Dassault Systèmes Simulia Corp, Providence, RI, USA, 2017.